DIAGNOSTIC NEURORADIOLOGY

Use of diffusion tensor imaging to identify similarities and differences between cerebellar and Parkinsonism forms of multiple system atrophy

Po-Shan Wang · Hsiu-Mei Wu · Ching-Po Lin · Bing-Wen Soong

Abstract

Introduction We performed diffusion tensor imaging to determine if multiple system atrophy (MSA)-cerebellar (C) and MSA-Parkinsonism (P) show similar changes, as shown in pathological studies.

Methods Nineteen patients with MSA-C, 12 patients with MSA-P, 20 patients with Parkinson disease, and 20 healthy controls were evaluated with the use of voxel-based morphometry analysis of diffusion tensor imaging.

Results There was an increase in apparent diffusion coefficient values in the middle cerebellar peduncles and cerebellum and a decrease in fractional anisotropy in the pyramidal tract, middle cerebellar peduncles, and white matter of the cerebellum in patients with MSA-C and MSA-P compared to the controls ($P<0.001$). In addition, isotropic diffusion-weighted image values were reduced in the cerebellar cortex and deep cerebellar nuclei in patients with MSA-C and increased in the basal ganglia in patients with MSA-P.

Conclusion These results indicate that despite their disparate clinical manifestations, patients with MSA-C and MSA-P share similar diffusion tensor imaging features in the infratentorial region. Further, the combination of FA, ADC and iDWI images can be used to distinguish between MSA (either form) and Parkinson disease, which has potential therapeutic implications.

Keywords Diffusion tensor imaging · DTI · Multiple system atrophy · MSA · Anisotropy

P.-S. Wang · H.-M. Wu · B.-W. Soong (✉)
Department of Neurology, School of Medicine,
National Yang-Ming University,
#155, Sec.2, Linung St., Peitou District,
112 Taipei, Taiwan
e-mail: bwsoong@ym.edu.tw

P.-S. Wang · B.-W. Soong
Department of Neurology, Taipei Veterans General Hospital,
Taipei, Taiwan

P.-S. Wang
Department of Neurology, Taipei Municipal Gan-Dau Hospital,
Taipei, Taiwan

P.-S. Wang · C.-P. Lin
Institute of Brain Science, National Yang-Ming University,
Taipei, Taiwan, Republic of China

H.-M. Wu
Department of Radiology, Taipei Veterans General Hospital,
Taipei, Taiwan

Introduction

Multiple system atrophy (MSA) is a form of sporadic spinocerebellar degeneration characterized by varying degrees of Parkinsonism, cerebellar ataxia, and autonomic dysfunction. It can be categorized by its dominant clinical features into two subtypes, MSA-C (cerebellar) and MSA-P (Parkinsonism) [1]. In the early phase of the illness, it is often difficult to distinguish MSA-P from Parkinson disease (PD). The emergence of noncerebellar symptoms, such as bulbar signs, autonomic dysfunction, and Parkinsonism, is often associated with a faster clinical course, shorter lifespan, and poorer prognosis in patients with MSA [2, 3]. Findings on conventional magnetic resonance (MR)

imaging are usually equivocal until later in the course of the disease and are poorly correlated with clinical severity. Although the two subtypes of MSA have very different clinical appearances, they share similar pathologic changes. A definitive diagnosis of MSA requires the identification of typical alpha-synuclein-positive glial cytoplasmic inclusions (GCIs) and selective neuronal loss in the basal ganglia, brainstem, and cerebellum upon neuropathologic examination [1, 4, 5]. Therefore, GCIs comprise a pathologic hallmark of MSA. The number of GCIs reflects the duration of illness and the severity of neuronal loss in MSA [4, 5]. Most GCIs are found in the white matter and appear to be associated with increased numbers of interfascicular oligodendroglial cells and loss of myelin staining [2].

Diffusion tensor imaging (DTI) is a novel MR technique that can generate images according to the characteristics of water diffusion within brain tissue [6]. The data can be segregated into anisotropic and isotropic clusters. Anisotropic clusters are believed to represent exclusively neural integrity, arising from random motions of water molecules restricted by myelinated axons in the white matter [7–9], and are generally characterized by fractional anisotropy (FA) [10]. In contrast, isotropic clusters represent cell bodies, and cellular units that exhibit isotropic diffusion are thought to represent the cytosol of glial and neuronal cells [11]. The apparent diffusion coefficient (ADC) is a quantitative index of diffusion-weighted imaging (DWI) that reflects water diffusivity within each MR voxel.

Several DTI studies have reported reduced anisotropy and increased diffusivity in patients with MSA. However, most of these studies have focused on anatomically defined regions of interest [12–15]. We aimed to investigate changes in FA, ADC, and isotropic DWI (iDWI) of different brain regions to ascertain whether these parameters are discriminatory between MSA-C and MSA-P or between MSA and PD. The ability to ascertain differences between these conditions could lead to improved diagnosis and treatment.

Methods

Subjects

This study included 19 patients with MSA-C, 12 with MSA-P, 20 with PD, and 20 healthy controls (Table 1). Diagnoses of MSA-C and MSA-P were made according to established guidelines [1]. The severity of ataxia was graded as follows: I, walking without assistance; II, walking with partial assistance; III, needing assistance walking; IV, needing assistance standing; and V, bedridden [16]. The severity of Parkinsonism was evaluated according to a modified Hoehn–Yahr staging system [17]. All subjects provided informed consent in accordance

Table 1 Demographic features of the study groups

	MSA-C (n=19)	MSA-P (n=12)	PD (n=20)	Control (n=20)	P value
Current age (years) [a]	54.8±9.1	63.0±12.7	68.9±11.8	52.4±19.5	<0.001
Disease duration (years) [a]	5.1±5.1	5.4±2.8	4.1±2.7	–	0.066
Gender [b]					
Male	8 (42.1)	4 (33.3)	15 (75.0)	10 (50.0)	0.034
Female	11 (57.9)	8 (66.7)	5 (25.0)	10 (50.0)	
Severity of ataxia [c]					
I	0 (0)	0 (0)	20 (100.0)	20 (100.0)	<0.001
II	19 (100.0)	9 (75.0)	0 (0)	0 (0)	
III	0 (0)	3 (25.0)	0 (0)	0 (0)	
IV	0 (0)	0 (0)	0 (0)	0 (0)	
V	0 (0)	0 (0)	0 (0)	0 (0)	
Modified Hoehn–Yahr [c]					
Stage 0	0 (0)	0 (0)	0 (0)	20 (100.0)	<0.001
1	0 (0)	0 (0)	0 (0)	0 (0)	
2	19 (100.0)	0 (0)	16 (80.0)	0 (0)	
3	0 (0)	9 (75.0)	4 (20.0)	0 (0)	
4	0 (0)	3 (25.0)	0 (0)	0 (0)	
5	0 (0)	0 (0)		0 (0)	

Severity of ataxia: *I* walking without assistance; *II* walking with partial assistance; *III* needing assistance walking; *IV* needing assistance standing; and *V* bedridden. *MSA-C* multiple system atrophy with cerebellar ataxia; *MSA-P* MSA with Parkinsonism; *PD* Parkinson disease

[a] Continuous data are expressed as mean ± standard deviation (SD)

[b] Categorical data are expressed as number (%) and were tested by chi-square test

[c] Ordinal data are expressed as mean ± standard deviation (SD) and were tested by Kruskal–Wallis test

Fig. 1 Apparent diffusion coefficient (ADC) values for patients with multiple system atrophy (MSA)-C or MSA-P. Statistical parametric mapping projection images on normalized magnetic resonance imaging slices illustrates regions of increased ADC values in patients with MSA-C (**a**) or MSA-P (**b**) compared to healthy controls. No changes in ADC values were observed in patients with Parkinson disease (PD) compared to healthy controls (**c**)
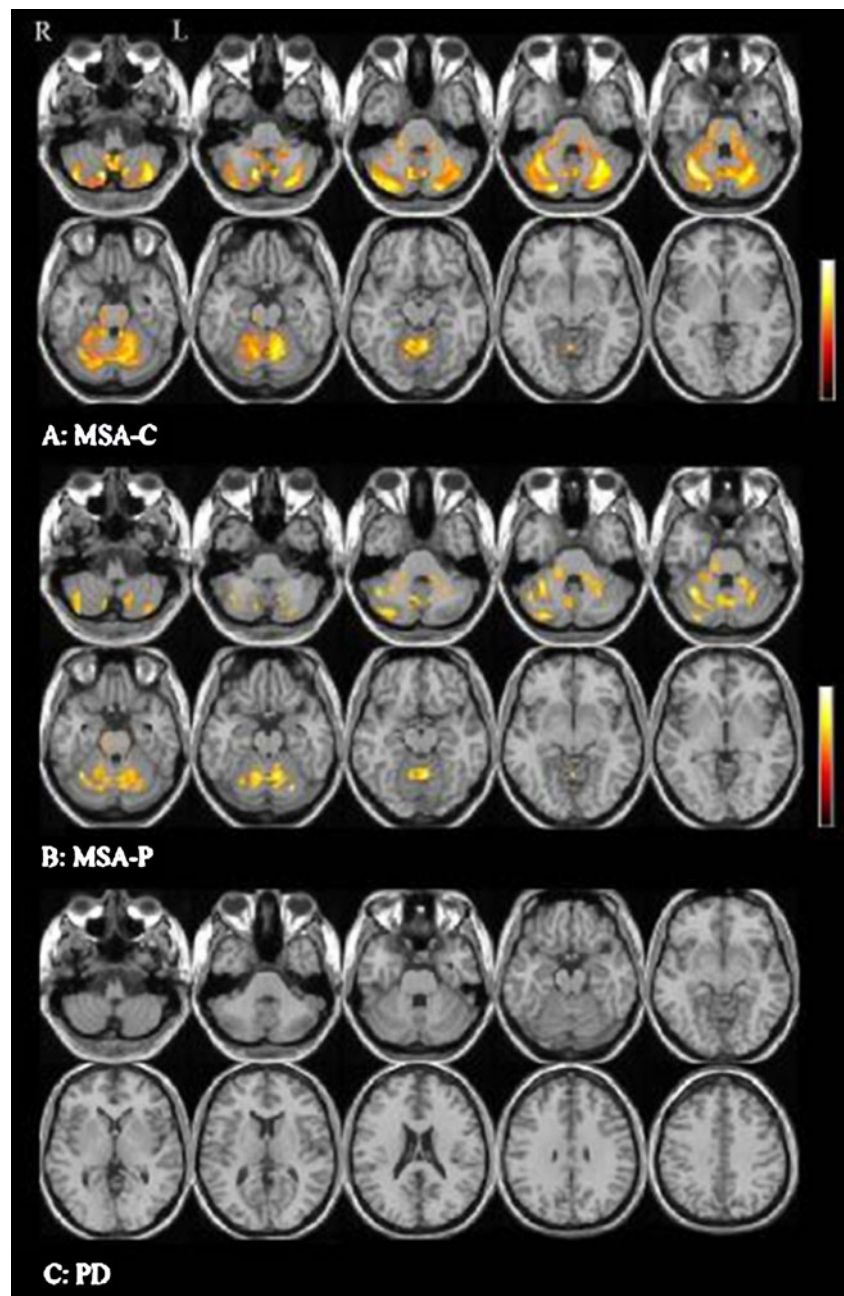
with our institutional review board policy (ethics approval number: VGHIRB No. 97-10-27A). The duration of illness was according to the patient's memory of the onset of earliest symptoms. This was asked at their first visit to the outpatient clinic (MRI was arranged at this time).

Magnetic resonance imaging and analysis

Data were acquired with a GE Signa 1.5 T LX MRI system (GE Healthcare, Milwaukee, WI, USA). Diffusion tensor imaging was performed using the single-shot, spin-echo, echo-planar imaging technique. The following DWI parameters were used: field of view=24×24 mm; matrix size=128×128; number of axial slices=52; slice thickness=3 mm; repetition time=15,000 ms; echo time=69.7 ms; diffusion-sensitizing pulse duration=23.5 ms (δ) with separation; b=1,000 s/mm^2; and number of diffusion-encoding directions=13. A circularly polarized head coil was used based on a T1-weighted MR sequence with the following parameters: axial slices=1.5 mm; echo time=5.5 ms; repetition time=14.4 ms; flip angle=20°; field of view=25 cm; matrix size=256×256; in-plane resolution=1×1 mm.

Table 2 Original MRI reports of MSA-C, MSA-P, PD and healthy controls

Data are expressed as number (%) and were tested by Fisher exact test

MSA-C multiple system atrophy with cerebellar ataxia; *MSA-P* MSA with Parkinsonism; *PD* Parkinson disease

	MSA-C (n=19)	MSA-P (n=12)	PD (n=20)	Control (n=20)	P value
Normal	1 (5.3)	1 (8.3)	13 (65.0)	15 (75.0)	<0.001
Cerebellar atrophy	18 (94.7)	4 (33.3)	0 (0)	0 (0)	<0.001
Hot cross bun sign	12 (63.2)	6 (50.0)	0 (0)	0 (0)	<0.001
Putaminal slits	3 (15.8)	5 (41.7)	0 (0)	0 (0)	<0.001
Cortical atrophy	0 (0)	7 (58.3)	7 (35.0)	5 (25.0)	0.001

Postprocessing strategies

The DWI data were used to construct isotropic images, anisotropic images, and an ADC map [18–20]. Fractional anisotropy is the ratio of the anisotropic component of the diffusion tensor to the entire tensor [18]. The apparent diffusion constant (ADCav) was calculated from the trace of the diffusion tensor (i.e., Dxx, Dyy, and Dzz) [18]. Isotropic images (iDWI) were obtained from the 13 diffusion-weighted images [18, 19]. The images assessed in this study were generated automatically by commercially available software (Functool; GE Medical Systems, Milwaukee, WI, USA).

The T1, ADC, FA, and iDWI images were analyzed using statistical parametric mapping (SPM) software (SPM2; Wellcome Department of Cognitive Neurology, Institute of Neurology, University College, London, United Kingdom). The gray matter and white matter of each T1 image were segmented using the SPM2 software, which automatically provided tissue segmentation of gray matter, white matter, and cerebrospinal fluid. All images were spatially normalized to a standard template (based on the Montreal Neurological Institute brain template) using a 12-parameter, affined transformation. To increase the signal-to-noise ratio and the validity of the statistical inference as well as to improve normalization, the spatially normalized images were smoothed by convolution using an isotropic gaussian kernel with 8-mm full width at half maximum [9].

Radiologic interpretation

The ADC, FA, and iDWI images were reviewed blindly. To control for experimental bias, one experienced neurologist and one experienced radiologist, without prior knowledge of the patient's clinical phenotype or other clinical information, read the images generated from raw ADC, FA, and iDWI data. They then reported if the images showed any of the following four features: increased cerebellar ADC values, decreased cerebellar FA values, decreased cerebellar iDWI values, or increased basal ganglia iDWI values. Changes in ADC, FA, and iDWI values in MSA-C and MSA-P were readily discernible on visual inspection of the DTI images (Fig. 1).

Table 3 Characteristic patterns of ADC, FA, and iDWI changes in MSA-C, as shown anatomically by three-dimensional Talairach coordinates

L left; *R* right; *MSA-C* multiple system atrophy with cerebellar ataxia; *ADC* apparent diffusion coefficient; *FA* fractional anisotropy; *iDWI* isotropic diffusion weighted images

Anatomic location	Talairach coordinate			Cluster level
	x	y	z	(Ke)
Regions of increased ADC value				
R cerebellum, posterior lobe, uvula	30	−63	−24	5,799
L cerebellum, anterior lobe, culmen	−32	−60	−26	
R cerebellum, posterior lobe, tuber	44	−73	−28	
L cerebellum, posterior lobe, tuber	−38	−65	−25	
R cerebellum, posterior lobe, tonsil	5	−50	−38	
L cerebellum, posterior lobe, tonsil	−4	−52	−40	
Regions of decreased FA value				
R pons	2	−19	−23	8,651
L pons	−5	−19	−24	
L cerebellum, anterior lobe, culmen	−28	−58	−24	
R cerebellum, posterior lobe, tonsil	28	−50	−33	
Regions of decreased isotropic value				
R cerebellum, posterior lobe, declive	8	−67	−20	1,342
R cerebellum, posterior lobe, pyramis	10	−69	−27	
R cerebellum, anterior lobe, culmen	−10	−35	−8	526
L cerebellum, anterior lobe, culmen	16	−42	−25	

Fig. 2 Fractional anisotropy (FA) values in patients with multiple system atrophy (MSA)-C or MSA-P. Statistical parametric mapping projection images on normalized magnetic resonance imaging slices illustrates regions of decreased FA values in patients with MSA-C (**a**) or MSA-P (**b**) compared to healthy controls. No changes in FA values were observed in patients with Parkinson disease (PD) compared to healthy controls (**c**)
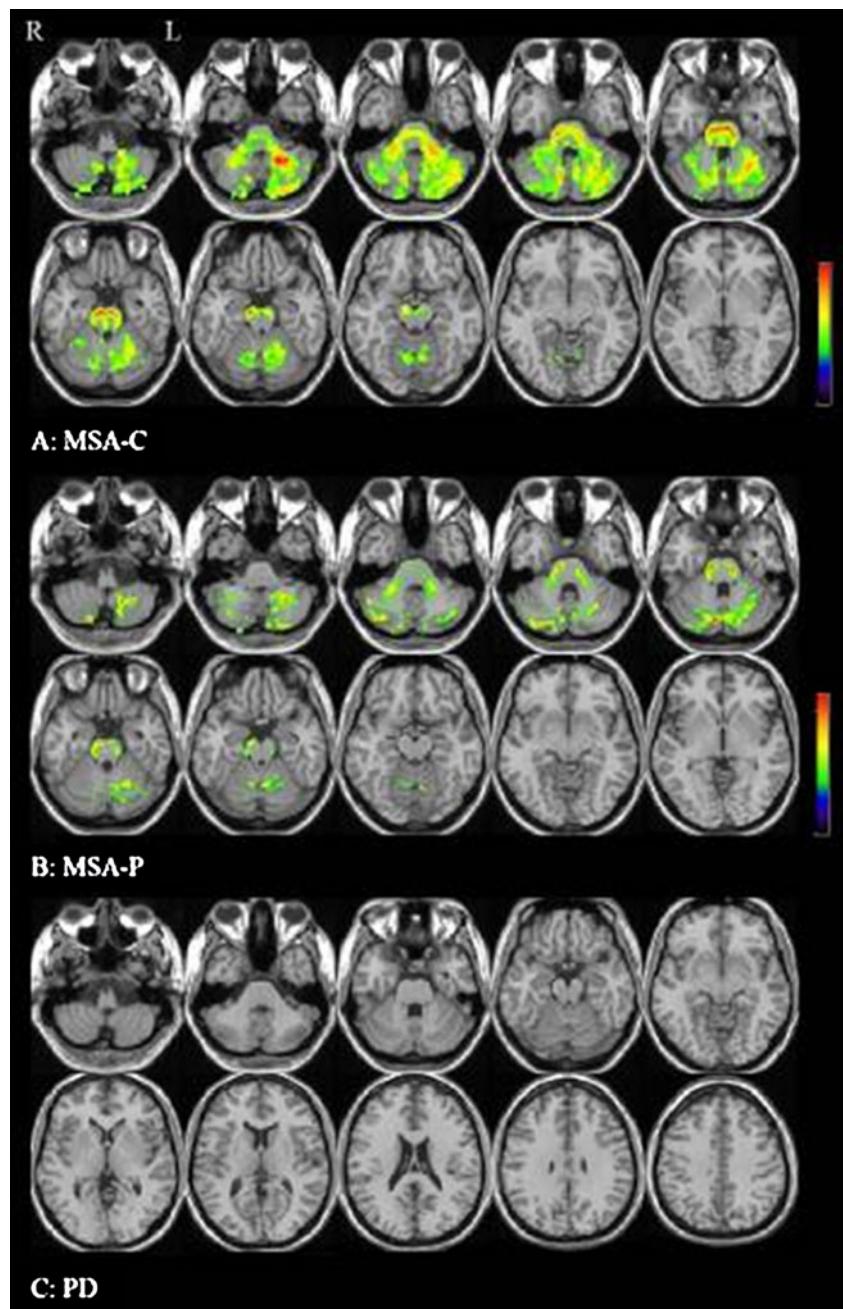

Statistical analysis

There are studies demonstrating the validity of applying voxel-based morphometry analysis to DTI [9, 21]. Normalized and smoothed ADC, FA, and iDWI images were compared statistically using a general linear model based on the gaussian field theory (analysis of covariance) in SPM. To minimize the impacts of duration of illness and current age, these variables were used as confounding nuisance covariates. Therefore, differences between the duration of illness would be statistically corrected, and the length of time since onset would not affect the patterns. Regional differences were considered significant only at an FDR corrected P value of <0.05 [9, 22–24]. The location of abnormalities was adjusted to three-dimensional Talairach coordinates by applying a nonlinear transformation, as described elsewhere (M. Brett, www.mrc-cbu.cam.ac.uk/Imaging/Common/mnispace.shtml).

Continuous data, including age, disease duration, and ordinal Hoehn–Yahr scale scores, as well as ataxia severity are expressed as mean ± standard deviation (SD) and were compared by Kruskal–Wallis test. Multi-

Fig. 3 Isotropic diffusion-weighted imaging (iDWI) values in patients with multiple system atrophy (MSA)-C or MSA-P. Statistical parametric mapping projection images on normalized magnetic resonance imaging slices illustrates regions of changes in iDWI values in patients with MSA-C (**a**) or MSA-P (**b**) compared to healthy controls. (**a**) MSA-C: Significant decrease of in iDWI values in the cerebellar cortex and deep cerebellar nuclei. (**b**) MSA-P: Increase of in iDWI values in the lentiform nuclei. No changes in iDWI values were observed in patients with Parkinson disease (PD) compared to healthy controls (**c**)
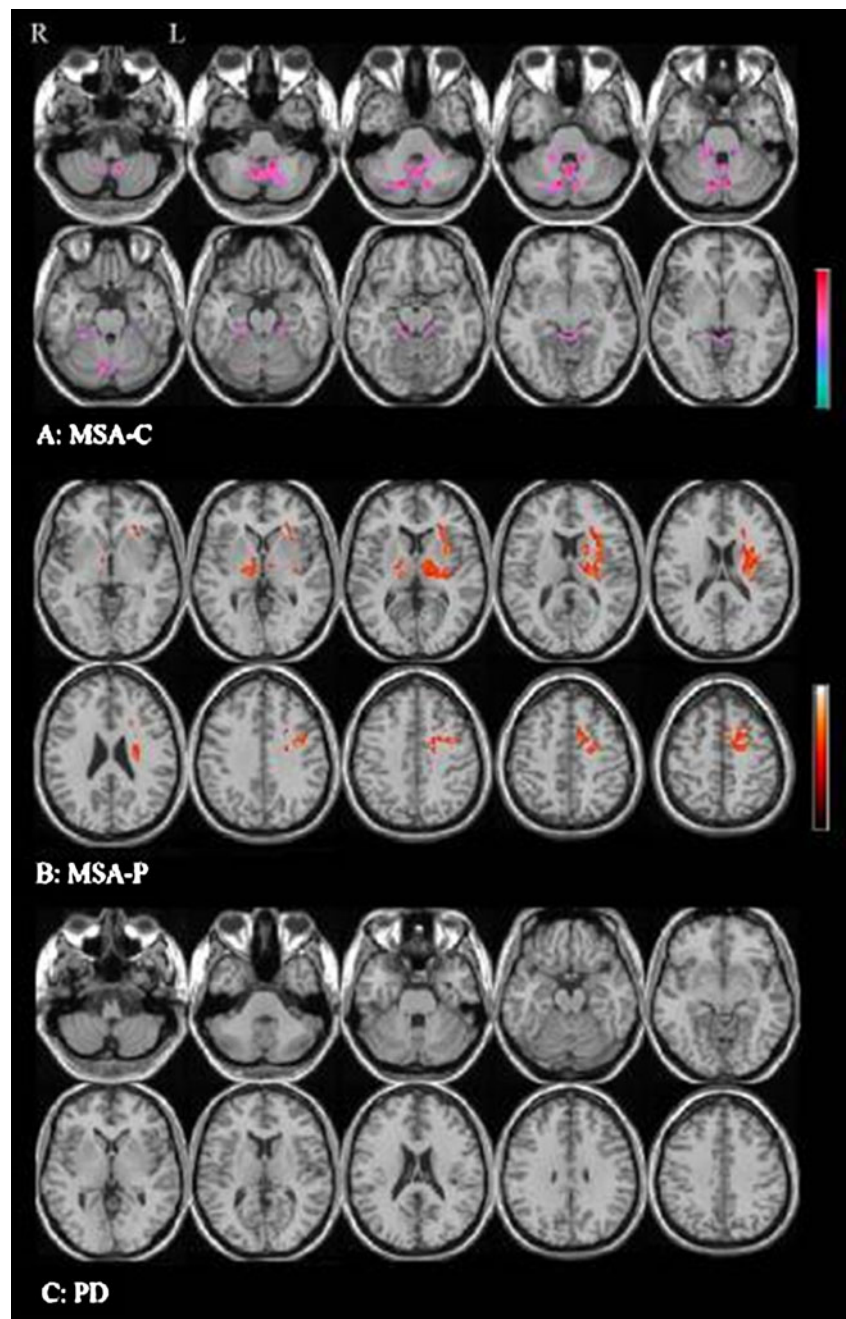
ple comparisons were performed with the Mann–Whitney test to determine differences between study groups if the results of Kruskal–Wallis test showed significant differences between groups. Categorical data are expressed as frequencies and percentages and were tested with the chi-square test or Fisher exact test. All statistical assessments were two-sided and evaluated at a 0.05 level of significance. Statistical analyses were performed with SPSS 15.0 statistics software (SPSS Inc., Chicago, IL, USA).

Results

Demographic features and clinical data are summarized in Table 1. There were no significant differences between groups with respect to disease duration. The groups showed statistically significant ($P<0.001$) differences with respect to current age, severity of ataxia, and modified Hoehn–Yahr stage, as well as gender ($P=0.034$). The MRI features of the T1- and T2-weighted images are summarized in Table 2. With respect to the most common feature, 18 patients in the

Table 4 Characteristic patterns of ADC, FA, and iDWI changes in MSA-P, as shown anatomically by three-dimensional Talairach coordinates

Anatomic location	Talairach coordinate			Cluster level
	x	y	z	(Ke)
Regions of increased ADC value				
R cerebellum, anterior lobe, culmen	30	−56	−22	1,840
L cerebellum, posterior lobe, declive	−26	−69	−15	
R cerebellum, posterior lobe, uvula	30	−79	−25	344
L cerebellum, posterior lobe, tonsil	−30	−60	−39	84
Regions of decreased FA value				
R cerebellum, posterior lobe, declive	8	−73	−22	2,008
L cerebellum, posterior lobe, declive	−8	−71	−22	
R pons	8	−21	−26	
L pons	−12	−25	−24	846
R cerebellum, posterior lobe, tonsil	30	−52	−33	
L cerebellum, posterior lobe, tonsil	−26	−58	−37	
Regions of increased isotropic value				
L frontal lobe, precentral gyrus, Brodmann area 6	−36	−4	35	731
L frontal lobe, medial frontal gyrus, Brodmann area 6	−8	8	51	
L claustrum	−34	4	5	1,144
R thalamus	12	−21	5	167

L left; *R* right; *MSA-P* multiple system atrophy with Parkinsonism; *ADC* apparent diffusion coefficient; *FA* fractional anisotropy; *iDWI* isotropic diffusion weighted images

MSA-C group (94.7%) showed cerebellar atrophy, and seven patients in the MSA-P group (58.3%) showed cortical atrophy. The groups showed statistically significant differences with respect to features ($P<0.001$ for all features).

By voxel-based analysis, a significant increase in ADC values in the middle cerebral peduncles (MCPs) and cerebellum and a decrease in FA in the pyramidal tract, MCPs, and white matter of the cerebellum were found in patients with MSA-C (Table 3, Figs. 1a and 2a) and MSA-P (Table 4, Figs. 1b and 2b) compared to the controls (cluster $P<0.001$). In addition, iDWI values were reduced in the cerebellar cortex and deep cerebellar nuclei in patients with MSA-C (Table 3, Fig. 3a) and increased in the basal ganglia (lentiform nuclei) in patients with MSA-P (Table 4, Fig. 3b). All of the voxels shown for MSA-C (ADC, FA, and iDWI) passed the threshold for corrected $P<0.05$. However, for MSA-P, only FA passed the threshold for corrected $P<0.05$. The ADC results of the infratentorial region in MSA-P passed the threshold for uncorrected $P<0.001$ but not corrected $P<0.05$. No statistically significant changes in FA (Fig. 2c), ADC (Fig. 1c), or iDWI values (Fig. 3c) were observed in patients with PD compared to normal control subjects.

At a threshold of corrected $P<0.05$, we found a significant reduction of gray matter in the cerebellar hemispheres in patients with MSA-C (Fig. 4). No statistically significant volume reduction in the white matter was observed in patients with MSA-C compared to the controls. No statistically significant atrophy of the gray matter or white matter was found in patients with MSA-P or patients with PD compared to controls.

The changes in ADC, FA, and iDWI values in patients with MSA-C or MSA-P were readily discernible on visual inspection of the DTI images (Table 5, Fig. 5). The reviewers reported increased cerebellar ADC values in 94.7% of patients with MSA-C and 75.0% of patients with MSA-P, as well as decreased cerebellar FA values in 94.7% of patients with MSA-C and 83.3% of patients with MSA-P. They also reported decreased cerebellar iDWI values in 57.9% of patients with MSA-C and increased iDWI values in the basal ganglia of 66.7% of patients with MSA-P. In contrast, 15.0% or less of healthy controls showed changes in ADC, FA, or iDWI. The groups showed statistically significant differences with respect to these values ($P<0.001$ for all values except for increased basal ganglia iDWI values ($P=0.009$)).

Discussion

We used 1.5 T DTI voxel-based morphometry to perform differential diagnostic categorization of 31 patients with MSA-C and MSA-P compared to patients with simple PD and healthy controls. Changes in ADC, FA, and iDWI values in patients with MSA-C or MSA-P, which were readily discernible on visual inspection of the DTI images (Table 5), showed a significant increase in ADC values in the MCPs and cerebellum and a decrease of FA in the pyramidal tract, MCPs, and white matter of the cerebellum in patients with MSA-C or MSA-P compared to the controls. In addition,
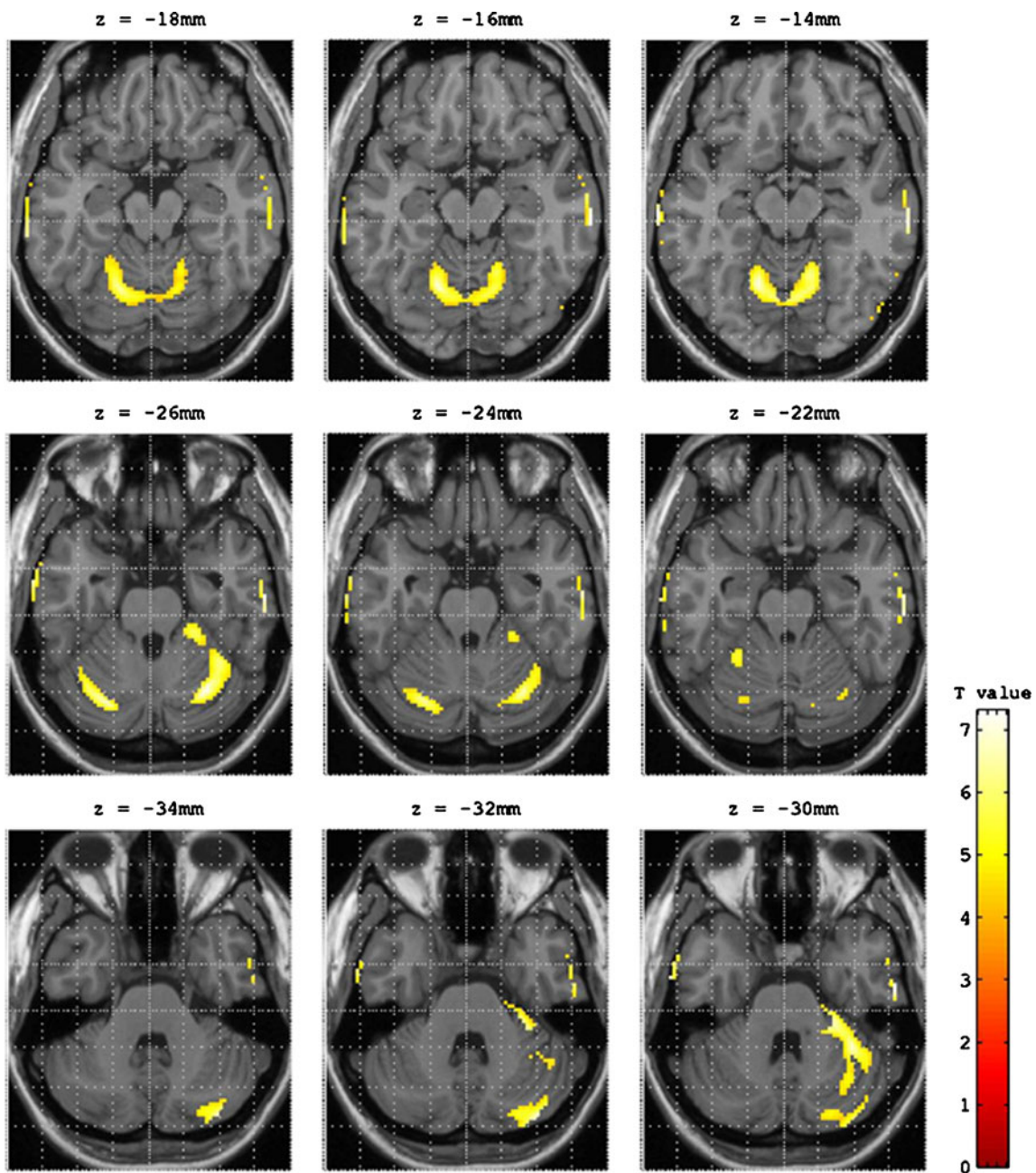
Fig. 4 Gray matter reduction in patients with multiple system atrophy (MSA)-C. Morphometric analysis was performed in patients with MSA-C compared to healthy controls. Gray matter was lost within the upper portions of the cerebellum

because iDWI values were significantly reduced in the cerebellar cortex and deep cerebellar nuclei in patients with MSA-C and increased in the basal ganglia of patients with MSA-P, these changes may be useful for the clinical diagnosis of MSA-C and MSA-P. Moreover, these novel findings allow for the differentiation of MSA (cerebellar or Parkinsonism form) from PD because patients with PD showed no significant changes in FA, ADC, or iDWI values compared to healthy controls.

Voxel-based morphometry analysis of brain MR images from patients with MSA-C has detected loss of gray matter in the cerebellar hemispheres and vermis [25] as well as loss of white matter in the pons, MCPs, mesencephalon, and frontotemporal areas [25–27]. In patients with MSA-P, volume loss occurs predominantly in the frontal, prefrontal, and insular cortices as well as the caudate nuclei, putamen, and midbrain [28]. These findings also appear strikingly similar to our observations.

Fig. 5 Raw diffusion tensor images of patients with multiple system atrophy (MSA)-C, MSA-P, Parkinson disease (PD), and healthy controls. From left to right, apparent diffusion coefficient (ADC), fractional anisotropy (FA) and isotropic diffusion-weighted images (iDWI) of the cerebellum and iDWI of the basal ganglia. (**a**) MSA-C: Increased ADC and decreased FA and iDWI values in the cerebellum, middle cerebral peduncles (MCPs), and pons compared to healthy controls. (**b**) MSA-P: Increased ADC and decreased FA values in the cerebellum, MCPs and pons, and increased iDWI values in the lentiform nuclei compared to healthy controls. (**c, d**) Both patients with PD and controls showed normal ADC, FA, and iDWI values
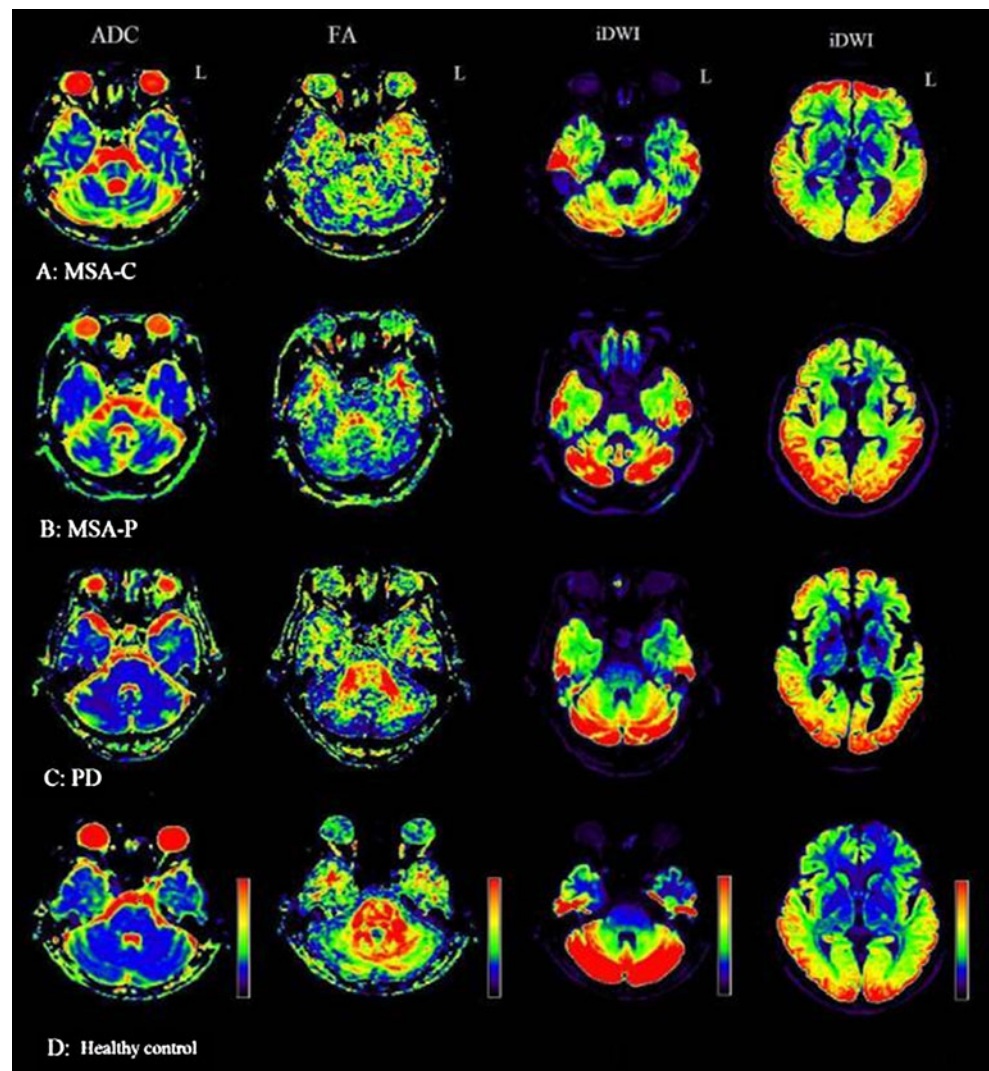
A definitive diagnosis of MSA requires the identification of typical alpha-synuclein-positive GCIs and selective neuronal loss in the basal ganglia, brainstem, and cerebellum upon neuropathologic examination [1, 4, 5]. Therefore, GCIs comprise a pathologic hallmark of MSA. The number of GCIs often reflects the duration of illness and the severity of neuronal loss in MSA [4, 5]. Most GCIs are found in the white matter and appear to be associated with increased numbers of interfascicular oligodendroglial cells and loss of myelin staining [4, 29]. Although GCIs are present in both MSA-C and MSA-P [4], the clinical phenotype correlates with GCI density, which is higher

Table 5 Changes of ADC, FA, and iDWI values in patients with MSA-C, MSA-P, PD, or healthy control subjects via visual inspection

	MSA-C (n=19)	MSA-P (n=12)	PD (n=20)	Controls (n=20)	P value
Increased cerebellar ADC values [a]	18 (94.7)	9 (75.0)	4 (20.0)	2 (10.0)	<0.001
Decreased cerebellar FA values [a]	18 (94.7)	10 (83.3)	5 (25.0)	3 (15.0)	<0.001
Decreased cerebellar iDWI values [b]	11 (57.9)	2 (16.7)	0 (0)	0 (0)	<0.001
Increased basal ganglia iDWI values [a]	8 (42.1)	8 (66.7)	6 (30.0)	2 (10.0)	0.009

MSA-C multiple system atrophy with cerebellar ataxia; *MSA-P* MSA with Parkinsonism; *PD* Parkinson disease; *ADC* apparent diffusion coefficient; *FA* fractional anisotropy; *iDWI* isotropic diffusion weighted images

[a] Data are expressed as number (%) and were tested by chi-square

[b] Data are expressed as number (%) and were tested by Fisher exact test

in the striatonigral region in MSA-P and higher in the oligodendrocyte progenitor cell (OPC) region in MSA-C [5], as well as the severity of neuronal cell loss. This may explain why increased ADC values in the MCPs and cerebellum and decreased FA values in the pyramidal tract, MCPs, and white matter of the cerebellum were observed in both MSA-C and MSA-P. Our present results showed that the changes in ADC in the infratentorial region in MSA-P was less than that in MSA-C; this finding may reflect differences in pathologic involvement and neuronal loss between MSA-C and MSA-P in the infratentorial region. Despite their disparate clinical manifestations, MSA-C and MSA-P shared similar DTI features in the infratentorial region. These distinctive features may reflect differences in GCI density and severity of neuronal loss in the striatonigral region, basal ganglia, and OPC regions.

In previous studies, iDWI has been useful in detecting tissue heterogeneities in patients, particularly stroke patients, which were otherwise undetectable with the use of other imaging techniques [11, 18, 20]. Patients with MSA-C or MSA-P have distinctively different iDWI features, and these differences may be exploited to differentiate MSA-C from MSA-P. Significant neuronal loss occurs in the putamen, caudate nuclei, and globus pallidus in MSA-P and in the pons, cerebellar hemispheres, cerebellar vermis, and inferior olivary nuclei in MSA-C [5]. The features of iDWI in MSA-C and MSA-P observed in the present study faithfully reflected these pathologic changes. The lower iDWI values in the cerebellar cortex and deep cerebellar nuclei in MSA-C patients may result from cytotoxic edema or a decrease in the cellular density of the brain parenchyma [11, 18, 20] and correspond well with findings of voxel-based morphometry studies [26, 27, 30]. In contrast, the higher iDWI values found in the basal ganglia (lentiform nuclei) in patients with MSA-P indicate that water molecules in the corresponding structures have a less restricted microstructural environment, suggesting a loss of cell-membrane integrity in response to cell injury [11, 18, 20]. Thus, the observed changes in iDWI values may imply different underlying pathologic changes in the basal ganglia in MSA-P compared to the deep cerebellar nuclei and cerebellar cortex in MSA-C.

Results of previous positron emission tomography studies have suggested that patients with MSA-C tend to exhibit glucose hypometabolism in the pons and cerebellum, whereas patients with MSA-P are more likely to exhibit glucose hypometabolism in the parietotemporal cortex, frontal cortex, and putamen [31]. Again, we identified features of iDWI in MSA-C and MSA-P that faithfully reflect these pathologic changes; iDWI values were significantly reduced in the cerebellar cortex and deep

cerebellar nuclei in patients with MSA-C and increased in the basal ganglia of MSA-P patients compared to control subjects.

A limitation of the present study was the limited number of patients, which made it difficult to match study groups in terms of size, age, and symptom duration. Further large-scale studies are warranted to evaluate the accuracy and sensitivity of the diagnosis of MSA according to DTI features.

In conclusion, differences in iDWI changes between MSA-P and MSA-C may result from similar pathologic changes involving different brain regions. In addition, despite their disparate clinical manifestations, patients with MSA-C or MSA-P share similar DTI features in the infratentorial region, which are distinctively different from those in patients with PD.

References

1. Gilman S, Wenning GK, Low PA, Brooks DJ, Mathias CJ, Trojanowski JQ, Wood NW, Colosimo C, Dürr A, Fowler CJ, Kaufmann H, Klockgether T, Lees A, Poewe W, Quinn N, Revesz T, Robertson D, Sandroni P, Seppi K, Vidailhet M (2008) Second consensus statement on the diagnosis of multiple system atrophy. Neurology 71:670–676

2. Gilman S, Little R, Johanns J, Heumann M, Kluin KJ, Junck L, Koeppe RA, An H (2000) Evolution of sporadic olivopontocerebellar atrophy into multiple system atrophy. Neurology 55:527–532

3. Wenning GK, Tison F, Ben Shlomo Y, Daniel SE, Quinn NP (1997) Multiple system atrophy: a review of 203 pathologically proven cases. Mov Disord 12:133–147

4. Wakabayashi K, Takahashi H (2006) Cellular pathology in multiple system atrophy. Neuropathology 26:338–345

5. Ozawa T, Paviour D, Quinn NP, Josephs KA, Sangha H, Kilford L, Healy DG, Wood NW, Lees AJ, Holton JL, Revesz T (2004) The spectrum of pathological involvement of the striatonigral and olivopontocerebellar systems in multiple system atrophy: clinico-pathological correlations. Brain 127:2657–2671

6. Bozzali M, Franceschi M, Falini A, Pontesilli S, Cercignani M, Magnani G, Scotti G, Comi G, Filippi M (2001) Quantification of tissue damage in AD using diffusion tensor and magnetization transfer MRI. Neurology 57:1135–1137

7. Beaulieu C (2002) The basis of anisotropic water diffusion in the nervous system - a technical review. NMR Biomed 15:435–455

8. Pierpaoli C, Barnett A, Pajevic S, Chen R, Penix LR, Virta A, Basser P (2001) Water diffusion changes in Wallerian degeneration and their dependence on white matter architecture. Neuroimage 13:1174–1185

9. Salmond CH, Menon DK, Chatfield DA, Williams GB, Pena A, Sahakian BJ, Pickard JD (2006) Diffusion tensor imaging in chronic head injury survivors: correlations with learning and memory indices. Neuroimage 29:117–124

10. Basser PJ, Pierpaoli C (1996) Microstructural and physiological features of tissues elucidated by quantitative-diffusion-tensor MRI. J Magn Reson B 111:209–219
11. Matsuzawa H, Nakayama N, Kwee IL, Nakada T (2005) Isotropic component trace analysis. J Neuroimaging 15:233–239
12. Kanazawa M, Shimohata T, Terajima K, Onodera O, Tanaka K, Tsuji S, Okamoto K, Nishizawa M (2004) Quantitative evaluation of brainstem involvement in multiple system atrophy by diffusion-weighted MR imaging. J Neurol 251:1121–1124
13. Schocke MF, Seppi K, Esterhammer R, Kremser C, Mair KJ, Czermak BV, Jaschke W, Poewe W, Wenning GK (2004) Trace of diffusion tensor differentiates the Parkinson variant of multiple system atrophy and Parkinson's disease. Neuroimage 21:1443–1451
14. Seppi K, Schocke MF, Mair KJ, Esterhammer R, Scherfler C, Geser F, Kremser C, Boesch S, Jaschke W, Poewe W, Wenning GK (2006) Progression of putaminal degeneration in multiple system atrophy: a serial diffusion MR study. Neuroimage 31:240–245
15. Yoshikawa K, Nakata Y, Yamada K, Nakagawa M (2004) Early pathological changes in the parkinsonian brain demonstrated by diffusion tensor MRI. J Neurol Neurosurg Psychiatry 75:481–484
16. Bang OY, Huh K, Lee PH, Kim HJ (2003) Clinical and neuroradiological features of patients with spinocerebellar ataxias from Korean kindreds. Arch Neurol 60:1566–1574
17. Kim SE, Choi JY, Choe YS, Choi Y, Lee WY (2003) Serotonin transporters in the midbrain of Parkinson's disease patients: a study with ^{123}I-β-CIT SPECT. J Nucl Med 44:870–876
18. Harris AD, Pereira RS, Mitchell JR, Hill MD, Sevick RJ, Frayne R (2004) A comparison of images generated from diffusion-weighted and diffusion-tensor imaging data in hyper-acute stroke. J Magn Reson Imaging 20:193–200
19. Zhang J, van Zijl PC, Mori S (2002) Three-dimensional diffusion tensor magnetic resonance microimaging of adult mouse brain and hippocampus. Neuroimage 15(892):901
20. Sotak CH (2002) The role of diffusion tensor imaging in the evaluation of ischemic brain injury - a review. NMR Biomed 15:561–569
21. Bruno S, Cercignani M, Ron MA (2008) White matter abnormalities in bipolar disorder: a voxel-based diffusion tensor imaging study. Bipolar Disord 10:460–468
22. Nestor PJ, Graham NL, Fryer TD, Williams GB, Patterson K, Hodges JR (2003) Progressive non-fluent aphasia is associated with hypometabolism centred on the left anterior insula. Brain 126:2406–2418
23. Wang PS, Liu RS, Yang BH, Soong BW (2007) Topographic brain mapping of the international cooperative ataxia rating scale. A positron emission tomography study. J Neurol 254:722–728
24. Wang PS, Liu RS, Yang BH, Soong BW (2007) Regional patterns of cerebral glucose metabolism in spinocerebellar ataxia type 2, 3 and 6: a voxel-based FDG-positron emission tomography analysis. J Neurol 254:838–845
25. Specht K, Minnerop M, Abele M, Reul J, Wüllner U, Klockgether T (2003) In vivo voxel-based morphometry in multiple system atrophy of the cerebellar type. Arch Neurol 60:1431–1435
26. Brenneis C, Boesch SM, Egger KE, Seppi K, Scherfler C, Schocke M, Wenning GK, Poewe W (2006) Cortical atrophy in the cerebellar variant of multiple system atrophy: a voxel-based morphometry study. Mov Disord 21:159–165
27. Specht K, Minnerop M, Müller-Hubenthal J, Klockgether T (2005) Voxel-based analysis of multiple-system atrophy of cerebellar type: complementary results by combining voxel-based morphometry and voxel-based relaxometry. Neuroimage 25:287–293
28. Brenneis C, Seppi K, Schocke MF, Müller J, Luginger E, Bösch S, Löscher WN, Büchel C, Poewe W, Wenning GK (2003) Voxel-based morphometry detects cortical atrophy in the Parkinson variant of multiple system atrophy. Mov Disord 18:1132–1138
29. Lantos PL, Papp MI (1994) Cellular pathology of multiple system atrophy: a review. J Neurol Neurosurg Psychiatry 57:129–133
30. Minnerop M, Specht K, Ruhlmann J, Schimke N, Abele M, Weyer A, Wullner U, Klockgether T (2007) Voxel-based morphometry and voxel-based relaxometry in multiple system atrophy-a comparison between clinical subtypes and correlations with clinical parameters. Neuroimage 36:1086–1095
31. Juh R, Pae CU, Lee CU, Yang D, Chung Y, Suh T, Choe B (2005) Voxel based comparison of glucose metabolism in the differential diagnosis of the multiple system atrophy using statistical parametric mapping. Neurosci Res 52:211–219